ISBN: 978-3-95450-248-6 ISSN: 2673-5490 doi: 10.18429/JACoW-IPAC2025-MOPM103

A PROPOSAL OF A MOMENTUM COLLIMATOR IN RHIC WARM SECTION FOR CONTROLLING EXPERIMENTAL BACKGROUND AT SPHENIX*

C. Liu†, D. Bruno, J. C. Brutus, A. Drees, H. Huang, G. Heppner, H. Lovelace,
C. Mi, M. Minty, G. Robert-Demolaize, D. Weiss
Brookhaven National Lab, Upton, NY, USA.

Abstract

One of the issues that the AuAu 100 GeV physics program in 2024 [1] in the Relativistic Heavy Ion Collider (RHIC) [2] encountered was background in the sPHENIX MVTX detector [3], which causes auto-recoveries and prevents continuous data taking. Beam studies and track simulations performed to understand the source of the background and potential measures to control it have led to the conclusion that off-momentum particle loss was an issue. This article will focus on a proposal of a momentum collimator in warm sections in RHIC to control the MVTX background. We will elaborate the selection of the locations for the collimator, the strategy of generating substantial horizontal dispersion there, the required additional powering scheme for selected quads and the optimization of the figure-of-merit for momentum collimation.

INTRODUCTION

The Monolithic Vertex Tracker (MVTX) [3] is a crucial component located at the center of the sPHENIX detector, designed to provide high-precision vertex tracking. It is desired to operate in a full-streaming mode, meaning the system continuously reads out data without an external trigger.

The MVTX consists of 48 staves arranged in three layers (Fig. 1), all centered at the interaction point (IP) and extending ±13.5 cm along the beam axis. Due to its streaming readout design, the MVTX is sensitive to excessive charge accumulation. If any of the staves become overloaded with charge, the entire stave enters an auto-recovery mode, a 20-second self-initiated reboot of the data acquisition process. During this period, no data from the recovering stave is available, leading to temporary loss of tracking information. The primary source of excessive charge deposition is the Yellow beam, which generates significantly higher hit rates compared to the Blue beam. In fact, 56 bunches in the Blue beam produce lower auto-recovery rates than one single Yellow bunch, highlighting the asymmetry in beam-induced effects on the detector. The MVTX auto-recovery display is shown in Fig. 1 where the red triangles correspond to staves in auto-recovery state.

The auto-recovery underscores the importance of carefully managing beam conditions and optimizing detector performance to minimize data loss due to auto-recovery events.The proposal for a momentum collimator is based on the hypothesis that the sPHENIX background originates primarily from off-momentum particles that deviate from the nominal beam energy and contribute to unwanted detector activity.

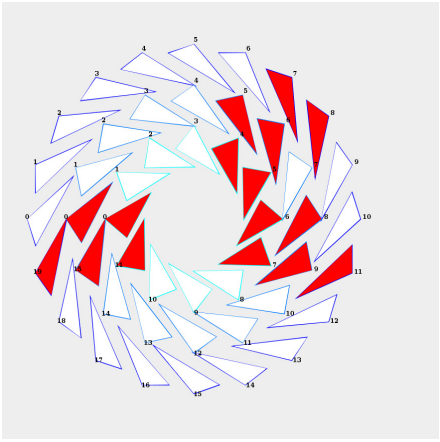

Figure 1: The cross-section of the MVTX detector. Each triangle represents one stave. The red triangles are the staves in auto-recovery mode, which takes 20 seconds before the stave can take data.

This assumption is supported by two key observations:

- The implementation of the pre-fire protection bump, which enhances the loss of off-momentum particles at dispersive arcs thus reduces the chance of loss near the sPHENIX detector, was found to reduce the MVTX auto-recovery rate.
- A controlled reduction in RF cavity voltage, which directly decreases the momentum spread of the circulating beam, also led to a decrease in MVTX auto-recovery events. This indicates a correlation between momentum spread and detector background, reinforcing the need for a mechanism to filter out off-momentum particles.

To reduce the off-momentum particle loss near the IR8 region and therefore the auto-recovery rate, the proposed strategy involves:

Creating dispersion in the warm section of the accelerator, where off-momentum particles are spatially separated from the core beam due to their energy deviation. Positioning

* Work supported by Brookhaven Science Associates, LLC under Contract No. DE-AC02-98CH10886 with the U.S. Department of Energy.
† cliu1@bnl.gov

ISBN: 978-3-95450-248-6 ISSN: 2673-5490 doi: 10.18429/JACoW-IPAC2025-MOPM103

a collimation mask in this dispersed region to selectively intercept off-momentum particles before they reach the interaction region, effectively acting as a momentum collimator. By implementing this approach, the goal is to reduce beam-induced background in sPHENIX, ensuring more stable detector operation and minimizing disruptions such as MVTX auto-recoveries.

LOCATION FOR DISPERSION BUMP

We would like to place the collimator in the warm sections because installing a collimator inside the cold section of RHIC is time-consuming and costly. By examining the design dispersion function in the warm sections, we identified specific locations where dispersion is more easily generated.

Figure 2 illustrates the beta function and the dispersion function in the IR12 region. These prime locations are typically at the triplet magnets and, in some cases, close to the Q4 magnet.

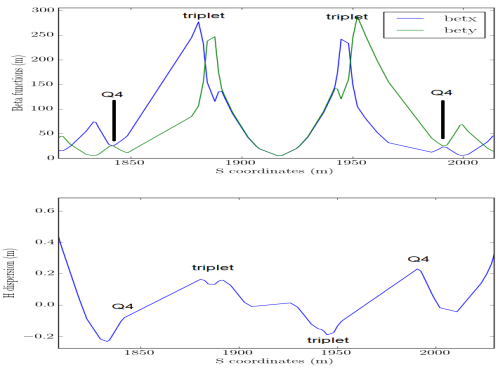

Figure 2: Upper plot: the β-functions in the IR12 region of the Yellow RHIC ring. Lower plot: the dispersion function in the IR12 region of the Yellow RHIC ring.

The suitability of a location for a momentum collimator depends on both the beta function and the dispersion. Mathematically, this can be expressed as a figure-of-merit, the ratio of the horizontal dispersion and the square root of the horizontal beta function, that quantifies the effectiveness of a given location. In the following analysis, we compare the figure-of-merit for two potential collimator placements: using the IR12 triplet magnet as the intended collimator location and using the IR12 Q4 magnet as the intended collimator location.

As shown in Fig. 3, it is evident that the Q4 location is preferable due to its higher figure-of-merit (> 0.1, which results from a smaller beta function. All the RHIC non-colliding IRs have a practically equivalent optical design at top energy so the conclusion applies to other IRs as well.

SELECTION OF QUADRUPOLES FOR DISPERSION GENERATION

The γ_t quadrupoles, located in the dispersive arcs and designed to facilitate fast crossing of transition energy by

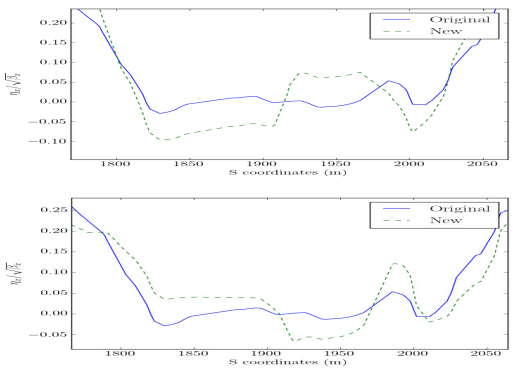

Figure 3: Upper plot: The figure-of-merit in the IR12 region with the triplet as the intended collimator location. Lower plot: The figure-of-merit in the IR12 region with the location near Q4 as the intended collimator location.

quickly changing the transition gamma [4, 5], are employed to generate dispersions. There are 48 individual quadrupole (Quad) magnets, which are powered by 12 power supplies.

The ideal tuning elements would be independent quadrupoles positioned at dispersive locations with a phase advance of $(2n + 1)\pi/2$ relative to the intended mask location [6]. Therefore, we need to pick the γ_t quads in the arcs on both sides of the selected Q4 magnet which meet the phase advance requirement. The authors studied the generated dispersion bump within the existing power supply limit for multiple IRs, and the associated constraints. The information is listed in Table 1.

Considering the figure-of-merit and space constraint, we chose the space near IR4 sector-4 Q4 magnet as the collimator location. The selected γ_t quadrupoles with their currents are listed in Table 2. These currents will be provided by additional power supplies.

FINALIZE THE SOLUTION WITH PRACTICAL CONSTRAINTS

As shown in the previous section, we selected the area near Q4 in IR4 as the collimator location, and used six γ_t quadrupoles on either side of IR4 to generate the dispersion bump. Additionally, Q8 and Q9, located at the beginning of the dispersion suppressor, are included in the matching to enhance the dispersion function at the collimator. As additional constraints, the tunes are kept constant and the chromaticities are kept at 2.

The dispersion around the Yellow ring, for the baseline lattice and for the lattice with dispersion bump at IR4, is shown in Fig. 4. The red box indicates the IR4 region, in which the peak to the right side is near the collimator location.

The figure-of-merit, for the baseline lattice and the lattice with dispersion bump at IR4, is shown in Fig. 5. As can be seen, the figure-of-merit at the collimator location is the highest among the warm sections. This enables the collimator with adjustable horizontal jaws on both sides to

ISBN: 978-3-95450-248-6 ISSN: 2673-5490 doi: 10.18429/JACoW-IPAC2025-MOPM103

Table 1: Comparison of Potential Locations for the Momentum Collimator

Location for Dispersion	Dispersion (m)	No. of PS	Space
IR12	+0.6	4	move equipment to make space, bake-out takes time
IR4	+0.5	6	Space available, bake-out takes less time
IR10	+0.5	4	Space is not available

Table 2: Selected γ_t Quadrupoles and Their Currents for IR4 Dispersion Bump

Magnet	Current (A)
yi3-qgt17	-47.5
yi3-qgt15	30.5
yi3-qgt13	47.5
yo5-qgt18	-41
yo5-qgt16	47.5
yo5-qgt14	44.5

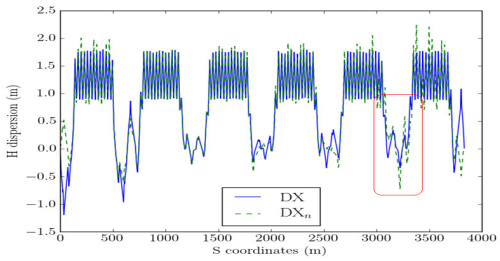

Figure 4: The dispersion bump at IR4 (red box) and resulting dispersion wave in the Yellow ring. The blue solid line depicts the baseline lattice, while the green dashed line depicts the lattice with dispersion bump at IR4.

intercept off-momentum particles before they scrape any other warm section locations.

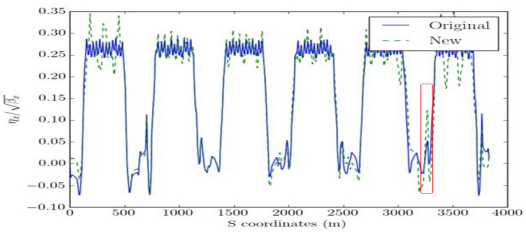

Figure 5: The figure-of-merit in the Yellow ring. The blue data is for the baseline lattice, while the green data is for the lattice with dispersion bump at IR4.

IMPLEMENTATION PLANS AND STATUS

Six re-purposed power supplies in alcoves nearby will provide the current and voltage to operate these γ_t quadrupoles as dispersion creators. The wiring of three of the six additional power supplies is shown in Fig. 6. As illustrated in Fig. 6, magnets Q11, Q13, Q15, and Q17 remain connected in series and are driven by the original Gamma Transition Power Supply (yi3-qgt-ps). To enhance post-ramp correction capability, three new power supplies—yi3-qgt13-ps, yi3-qgt15-ps, and yi3-qgt17-ps—have been integrated into the system (indicated by the green rectangular box), with associated cabling routed through the tunnel cable tray (shown as pink wires in the diagram).

During the energy ramp, the original yi3-qgt-ps continues to execute the gamma transition jump as before. Initially, all output relays for the new power supplies remain open, keeping them isolated from the magnet circuit. After the beam reaches flat-top energy, the relays for yi3-qgt13-ps, yi3-qgt15-ps, and yi3-qgt17-ps close, enabling each unit to inject additional corrective current into the corresponding Q13, Q15, and Q17 magnets. A LEM module is used to monitor the total current delivered to each magnet and provides an interlock to prevent over-current through the current feedthroughs from the warm to cold sections. The control of the relay states and the LEM monitoring modules are managed by a newly designed control/interface chassis.

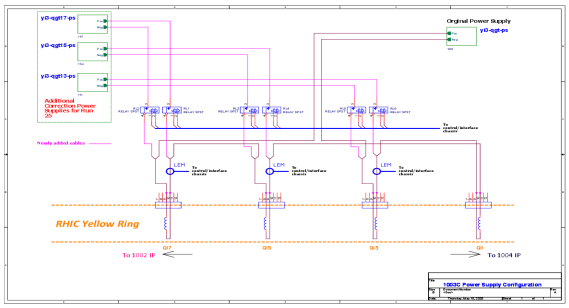

Figure 6: The wiring scheme for the γ_t quadrupoles chosen for generating dispersion at IR4. The additional power supplies are connected to the chosen magnets by relays which engages at top energy.

The existing Blue Mask has been removed and relocated near the Q4 magnet in Sector 4. This relocation process necessitates two bake-out procedures to ensure system integrity and maintain ultra-high vacuum conditions. To accommodate this modification, associated diagnostic instrumentation, including pin diodes and the beam loss monitor, will be re-positioned accordingly. These adjustments are critical for maintaining accurate beam loss measurements and optimizing machine protection.

Additionally, successful implementation of this relocation requires close collaboration with the Controls and Instrumentation group. Their role includes overseeing low-voltage system management, installing and configuring updated cabling, and ensuring proper signal acquisition and processing via the scalar board within a Field Electronic Controller (FEC).

ISBN: 978-3-95450-248-6 ISSN: 2673-5490 doi: 10.18429/JACoW-IPAC2025-MOPM103

REFERENCES

[1] K. Hock *et al.*, "RHIC Au operation in Run24", presented at the IPAC'25, Taipei, Taiwan, Jun. 2025, paper MOPM001, this conference.

[2] M. Harrison, S. Peggs, T. Roser, "The RHIC accelerator", *Annu. Rev. Nucl. Part. Sci.*, Vol. 52, pp. 425–469, 2002. doi:10.1146/annurev.nucl.52.050102.090650

[3] K. Hock *et al.*, "sPHENIX Backgrounds", presented at RHIC Retreat 2024, Upton NY. https://indico.bnl.gov/event/24848/contributions/97461/attachments/58573/100572/sPHENIX_Background_RHIC_Retreat.pdf

[4] S. Peggs, S. Tepikian, and D. Trbojevic, "A First Order Matched Transition Jump at RHIC", in *Proc. PAC'93*, Washington D.C., USA, Mar. 1993, pp. 168–171.

[5] J. Kewisch and C. Montag, "Commissioning of a First-Order Transition Jump in RHIC", in *Proc. PAC'03*, Portland, OR, USA, May 2003, paper TPPB035, pp. 1694–1696.

[6] C. Liu, J. Kewisch, H. Huang, and M. Minty, "Minimization of spin tune spread for preservation of spin polarization at RHIC", *Phys. Rev. Accel. Beams*, vol. 22, no. 6, Jun. 2019. doi:10.1103/physrevaccelbeams.22.061002